[Article ID] 1003- 6326(2002)04- 0702- 05

Characterization of sputter-deposited TiPdNi thin films①

TIAN Qing-chao(田青超)[1, 2], WU Jian-sheng(吴建生)[1]
(1. Key Laboratory of Ministry of Education for High Temperature Materials and Tests, School of Materials Science and Engineering, Shanghai Jiaotong University, Shanghai 200030, China;
2. Testing Center, Baoshan Iron & Steel Co., Ltd, Shanghai 201900, China)

[Abstract] TiPdNi thin films were prepared by magnetron sputtering onto unheated glass and silicon substrate. Atomic force microscope, energy-dispersive X-ray microanalyzer, X-ray diffractometer, differential scanning calorimeter and optical microscope were used to characterize the films. It is found that the surface morphology of the films change during the sputtering process and a shift of about 3% Ti(mole fraction) content from the center to the edge of the substrate occurs. The freestanding as-deposited films undergo crystallization followed by three kinds of cooling conditions. For all these heat-treated films, B2 → B19 → B19′ two-stage phase transformation takes place. Many Ti_2Ni and Ti_2Pd type of precipitates are detected in the films. The constraint films on silicon substrate are crystallized at high temperature. After crystallization, the films show a two-way shape memory effect.

[Key words] TiPdNi; thin film; sputter deposition; martensitic transformation; shape memory effect
[CLC number] TG 139.6 [Document code] A

1 INTRODUCTION

Shape memory thin films are regarded as one of the most promising materials for micro electromechanical system (MEMS) because it provides large output force per unit volume and works as both a structural and a functional component. Deposited TiNi thin films are intensely investigated and are widely used at present. Comparing with the conventional shape memory thin films, TiPdNi films exhibit higher phase transformation temperature, respond quickly to the efficient thermal exchange, and thus have received much attention for fabricating microactuators. It is important to study the phase transformation behavior because the shape memory effect is generally realized through the transformation process. In $Ti_{50}Pd_xNi_{50-x}$ alloys, phase transformation has been studied by many authors[1, 2]. It is known that the transformation sequence is changed from B2 → B19′ through B2 → R → B19′ to B2 → B19 → B19′, and then into B2 → B19 as the Pd content increases. Here, B2 refers to the high temperature austenite phase (CsCl type structure), while B19 and B19′ to the orthorhombic and monoclinic martensite, respectively. According to our previous work concerning the bulk $Ti_{50+x}Pd_{30}Ni_{20-x}$ alloys, both the B2 → B19 and the B2 → B19 → B19′ transformations can be retained through various heat treatment conditions[3]. In the films sputtered from $(TiPd)_{50}(TiNi)_{50}$ target[4], it is believed that a mixture of B19 and B19′ phases would exist at low temperature. It is therefore necessary to obtain a clear understanding of the phase transformation behavior in TiPdNi thin films.

2 EXPERIMENTAL

$Ti_{50.6}Pd_{30}Ni_{19.4}$ ingot was made by arc melting 99% Ti, 99% Ni and 99.9% Pd on a water-cooled copper mould under a controlled protective argon atmosphere. One ingot was remelted four times, and then homogenized in vacuum at 1 000 ℃ for 5 h. Finally, the ingot was hot-rolled into 1 mm thick plate at 800 ℃. A target with gauge size of d78 mm × 1 mm was spark cut followed by mechanically polishing. Films were formed by radio frequency (RF) magnetron sputtering onto unheated glass and silicon substrates in Ar gas at 0.6 Pa. The base pressure in the deposition system was of the order of 10^{-4} Pa. RF power was 200 W and the substrate-target distance was about 50 mm. Energy-dispersive X-ray microanalysis was employed to measure the composition of the films. In order to observe the surface morphology of film with different sputtering time, atomic force microscope (AFM) was used. The as-deposited thin films were peeled off from the glass substrate, and then were crystallized under the protection of Ti plate at 750 ℃ for 1 h in three quartz capsules filled with argon. Finally, the individual capsule experienced air-cooling (Ⅰ), furnace cooling (Ⅱ), and aging at 450 ℃ for 18 h (Ⅲ), respectively. The films on silicon substrate were also crystallized under the protection of Ti plate at 750 ℃ for 1 h in vacuum. The films were peeled off and curled automatically after the treatment. A curled film was heated to 300 ℃

① [Foundation item] Project (00JC14055) supported by the Science and Technology Commission of Shanghai Municipal Government
[Received date] 2001- 10- 08

to observe its shape changes by using an optical microscope.

X-ray diffraction (XRD) measurements were performed using a Rigaku D/max 2 550 V diffractometer with a CuK_α radiation. The phase transformation temperatures of the bulk target and the thin films were determined by differential scanning calorimetry (DSC) using a Perkin-Elmer model Pyris I calorimeter. The masses of the specimens II, III and I were 1.4 mg, 5.3 mg and 3.7 mg, respectively. The heating (cooling) rate for all the specimens was 40 ℃/min.

3 RESULTS

3.1 Deposition process

Fig. 1 shows the evolution of surface morphology of the as-deposited thin films with different sputtering time. Figs. 1(a) ~ (e) correspond to 30 s, 1 min, 5 min, 10 min and 30 min, respectively. It can be found that the film surface is very rough at the initial stage of deposition, and some pinnacles homogeneously scatter over the surface (as shown in Fig. 1(a)). The prolonging of the sputtering time causes a very dense distribution of pinnacles (as shown in Fig. 1 (b)) which grow and merge with each other after 5 min deposition, leaving holes in the film surface (as shown in Fig. 1(c)). The sputtered atoms go into the holes in the following deposition process, as a result, the holes are nearly removed after 10 min deposition (as shown in Fig. 1(d)) and after 30 min deposition the surface is very smooth (as shown in Fig. 1(e)).

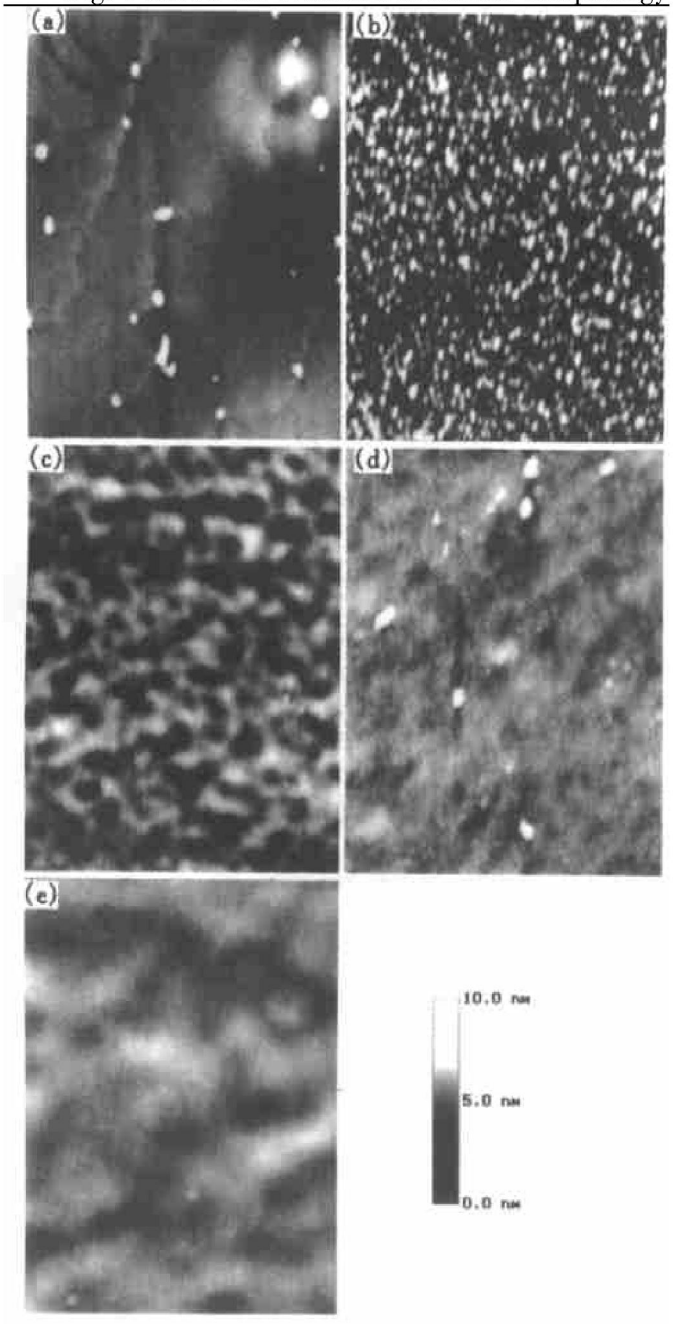

Fig. 1 Surface morphology of films with different sputtering time
(a) —30 s; (b) —1 min; (c) —5 min; (d) —10 min; (e) —30 min

3.2 Film composition

It has been found that the transformation temperature of TiNi-based alloy is very sensitive to the Ti content and can be changed greatly even by a slight fluctuation of the Ti content less than 1% (mole fraction)[5]. Fig. 2 shows the distribution of Ti content on the substrate, in which the Ti content varies from 53.41% at the center to 50.15% (mole fraction) at the edge. Obviously, this Ti content variation would cause a various transformation temperature distribution in micro-region in the films. In order to eliminate the inhomogeneity of the film composition, a long-time (18 h) aging treatment (specimen III) is necessary.

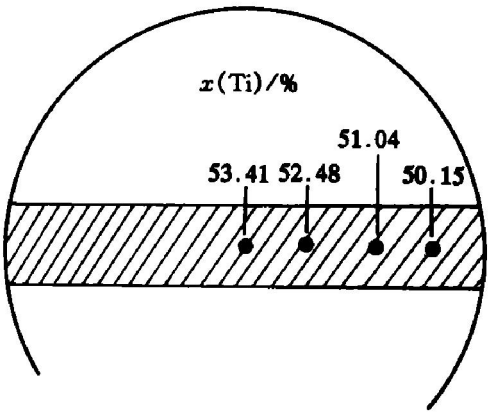

Fig. 2 Distribution of Ti content

3.3 Phase constitution

The as-deposited thin films with thickness about 2 μm were amorphous as revealed by XRD patterns. The films crystallized at 750 ℃ then aged at 450 ℃ consisted of four phases, i.e., the martensite phases B19 and B19′, together with the precipitates Ti_2Ni and Ti_2Pd, as shown in Fig. 3.

3.4 Phase transformation

The bulk target shows obviously the B2 → B19 one-stage phase transformation. The characteristic temperatures were determined as follows: the start and finish temperatures of martensite transformation

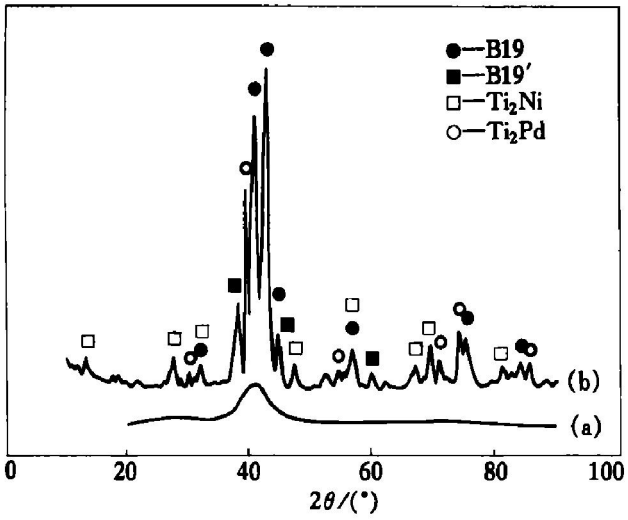

Fig. 3 XRD patterns of as-deposited and crystallized thin films
(a) —As deposited; (b) —Crystallization at 750 ℃ for 18 h

are 269.5 ℃, 213.7 ℃, and those of austenite transformation are 243.5 ℃ and 288.7 ℃ respectively.

Fig. 4 shows the heat flow curves of the three kinds of crystallized thin films under different cooling conditions. Obviously, multi-stage phase transformation took place, and the transformation temperature was lower than that of the bulk target.

3.5 Shape memory effect

The two-way shape memory effect the film is shown in Fig. 5. The film underwent three stages on both heating and cooling process: room temperature (RT), 200 ℃ and 300 ℃. Without any external biasing the film initially curled, then uncurled when being heated, and curled when being cooled down to room temperature. The shape recovery effect is perfect.

4 DISCUSSION

4.1 Sputtering factors

Ar gas pressure, RF power, substrate-target distance, substrate temperature and alloy composition of the target used are important sputtering factors affecting the quality of the films. The films prepared at a low Ar gas pressure or a high RF power exhibit a flat and featureless structure, while the films show a columnar structure under the reverse conditions[6]. Therefore, moderate pressure and power were adopted in the present paper. The distance between substrate and target strongly influences the deposition rate and uniformity of composition of the film on the substrate surface. Shortening the distance enhances the deposition rate; while the uniformity of composition degenerated[7]. In our experiment, the distance was fixed at 50 mm. As to the influence of the substrate temperature, it was reported that the as-grown films were crystalline when sputtering at elevated temperature[4].

Generally, the sputtering yield (number of

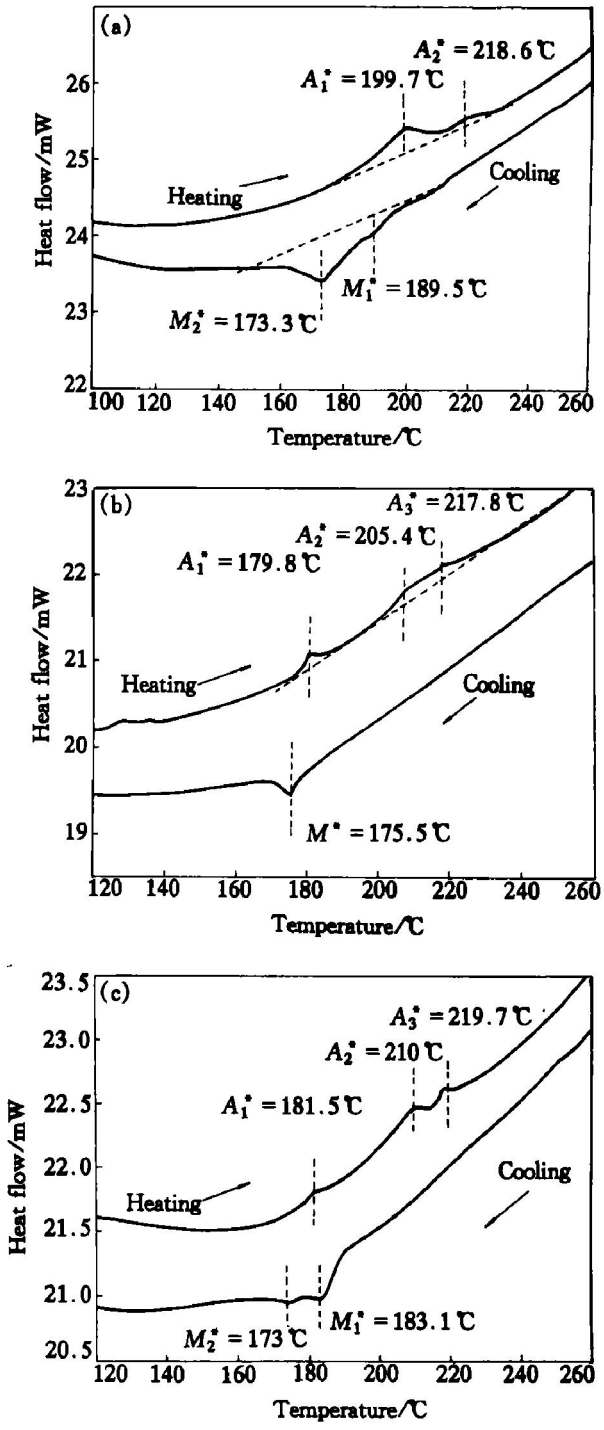

Fig. 4 DSC curves of films crystallized at 750 ℃ followed by
(a) —Aging for 18 h; (b) —Furnace cooling; (c) —Air-cooling

atoms sputtered per Ar ion) for Ti is lower than that for Ni or that for Pd. Therefore, the composition of the target is very important. In order to obtain an ideal film composition, off-stoichiometric $Ti_{50.6}Pd_{30}Ni_{19.4}$ target was prepared. It can be seen from Fig. 2 that a shift of about 3% Ti (mole fraction) content from the center to the edge of the substrate occurs in the films, which is because the angular flux distribution for Ti is wider than that for Ni and Pd. A non-linear relationship of the composition of the films with that of the target exists.

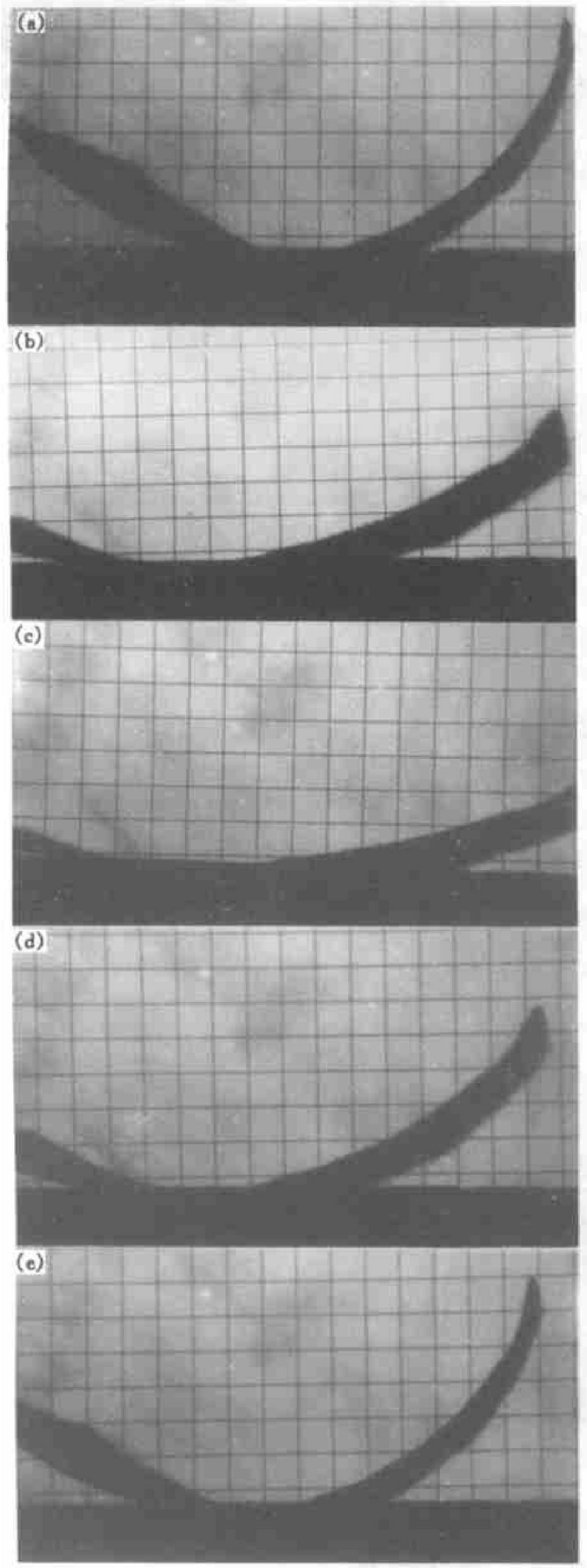

Fig. 5 Optical observation on two-way shape memory effect
(a) —RT; (b) —200 ℃; (c) —300 ℃; (d) —200 ℃; (e) —RT

4.2 Transformation characteristic

According to the XRD patterns of the film, B19 and B19′ coexisted at room temperature. It shows that there exhibit the B2 → B19 one-stage and the B2 → B19 → B19′ two-stage phase transformations. It is suggested that the two kinds of transformations are responsible for the peaks(valleys) in the DSC curves as discussed below.

Fig. 4(a) indicates a two-stage phase transformation. Obviously, the B2 → B19 → B19′ two-stage transformation should take place. Because the B19 and B19′ phases exist at room temperature, it can be deduced that the B19 → B19′ transformation is incomplete. In other words, the overlapping heat flow peaks can be regarded as a combining thermal effect of both B2 → B19 and B2 → B19 → B19′ phase transformations.

Fig. 4(b) and 3(c) show similar peaks(valleys) but are different from Fig. 4(a), especially in the heating process. A transformation peak (A_1^*) lying near 180 ℃ exists for the crystallized films experienced both furnace cooling (as shown in Fig. 4(b)) and air-cooling (as shown in Fig. 4(c)), and the cooling rates are approximately 75 ℃/ h and 75 ℃/ min, respectively. However, other two overlapping peaks (A_2^*, A_3^*) (valleys(M_1^*, M_2^*)) correspond to each other for the three kinds of specimens.

It is considered that the A_1^* peak in the DSC curves of specimen Ⅱ and Ⅰ correspond to the B19 → B2 one-stage phase transformation, while the overlapping peaks to the B19′ → B19 → B2 two-stage transformation.

The presupposition is the coexistence of B19′ and B19 phase at low temperature, as well as the activation energy for nucleus formation. It is known that the lattice distortion in B19′ martensite is more severe than that in B19 martensite. As a reasonable deduction, the activation energy for B19 → B2 transformation is lower than that for B19′ → B2 transformation. Therefore, the A_1^* peak should correspond to the B19 → B2 transformation. During the transformation process of B19′ → B2, B19 acts as media in the lattice distortion governed by the principle of lowest energy in the system. However, there only exists two overlapping peaks during the cooling process. This phenomenon is also understandable. That is, the two peaks correspond to the B2 → B19 → B19′ transformation, while B19 → B19′ transformation is incomplete, leaving the B19′ phases in the films.

However, the individual B19 → B2 transformation peak (near 180 ℃) does not appear in the DSC curves for specimen Ⅲ(as shown in Fig. 4(a)). In fact, it is the result of inhomogeneity of the film composition. It can be seen from Fig. 2 that much precipitation occurred in the films experienced long time aging according to the relatively high peaks in the XRD pattern. The precipitates, i. e., Ti_2Ni and Ti_2Pd, will introduce the internal stress, which will make

the composition of the matrix shift toward the equiatomic $Ti_{50}(NiPd)_{50}$, and thus eliminate the effect of composition inhomogeneity to a certain degree. At the same time, the lattice distortion of B19′ is not so severe as before. As a result, the difference of the activation for nucleus formation between B19 and B19′ is not so distinct. Therefore, the transformation of B19 and B19′ to B2 may proceed simultaneously. An investigation on the bulk TiPdNi alloy indicates that the elastic modulus of B19 and B2 is much lower than that of B19′[3], which means a higher activation for nucleation of B19′ than that of B19 is necessary in the B2 → B19 → B19′ transformation process. A careful inspection to the DSC curve revealed that, therefore, the low temperature peak was much higher than the high temperature one in Fig. 4(a).

4.3 Two-way shape memory effect

The films on silicon substrate were protected by Ti plate in the crystallization process. Therefore, in fact, the films were in constraint. The constraint produced preferentially oriented precipitates which have an intrinsic stress field around them, causing the two-way shape memory effect to appear. After crystallization, the films were peeled off due to high internal stress caused by nucleation and growth of crystal grains in the original amorphous matrix. The two-way shape memory effect, useful for miniaturizing and simplifying microactuators, is usually obtained by training. This paper provides an immediate method to realize it in the film preparation process.

5 CONCLUSIONS

1) In the specific sputtering conditions, the film surface becomes smooth after being deposited for 30 min. The composition of the thin films was dependent on the positions in the substrate, a shift of about 3% Ti (mole fraction) content from the center to the edge of the substrate occurred.

2) The phase transformation temperatures of $Ti_{50.6}Pd_{30}Ni_{19.4}$ target were much higher than that of its thin films. B19′ and B19 phases coexisted in the thin films, together with the Ti_2Ni and Ti_2Pd type of precipitates. Both the B19 → B2 one-stage and the B19′ → B19 → B2 two-stage phase transformation took place in all the crystallized films followed by different cooling conditions.

3) A two-way shape memory effect was observed after the films were crystallized under constraint.

[REFERENCES]

[1] Matveeva N M, Kovneristyi Y K, Savinov A S, et al. Martensitic transformations in the TiPd-TiNi system [J]. J Physique, 1982, 43: 249–251.

[2] Lo Y C, Wu S K. Compositional dependence of martensitic transformation sequence in $Ti_{50}Ni_{50-x}Pd_x$ alloys with $x <$ at. 15% [J]. Scripta Metall Mater, 1992, 27: 1097–1102.

[3] Tian Q C, Wu J S. Phase transformation behaviour and microstructure of $Ti_{51}Pd_{30}Ni_{19}$ alloy [J]. Z Metakd, 2001, 5: 436–440.

[4] Mathews S, Li J, Su Q, et al. Martensitic transformation in thin-film $(TiPd)_{50}(TiNi)_{50}$ [J]. Phil Mag Lett, 1999, 79: 265–272.

[5] Tian Q C, Wu J S. The elastic behavior of $Ti_{50+x}Pd_{30}Ni_{20-x}$ high-temperature shape memory alloys [J]. Acta Metall Sinica, 2001, 6: 658–664.

[6] Miyazaki S, Ishida A. Martensitic transformation and shape memory behavior in sputter-deposited TiNi-based thin films [J]. Materials Science and Engineering A, 1999, 273–275: 106–133.

[7] Ohta A, Bhansali S, Kishimoto I, et al. Novel fabrication technique of TiNi shape memory alloy film using separate Ti and Ni targets [J]. Sensors and Actuators, 2000, 86: 165–170.

(Edited by YANG Bing)